Two-Dimensional Computational Fluid Dynamics and Conduction Simulations of Heat Transfer in Window Frames with Internal Cavities - Part 1: Cavities Only

Arild Gustavsen, Christian Kohler, Dariush Arasteh and Dragan Curcija

ABSTRACT

Accurately analyzing heat transfer in window frame cavities is essential for developing and characterizing the performance of highly insulating window products. Window frame thermal performance strongly influences overall product thermal performance because framing materials generally perform much more poorly than glazing materials. This paper uses Computational Fluid Dynamics (CFD) modeling to assess the accuracy of the simplified frame cavity conduction/convection models presented in ISO 15099 and used in software for rating and labeling window products. (We do not address radiation heat-transfer effects.) We examine three representative complex cavity cross-section profiles with varying dimensions and aspect ratios. Our results support the ISO 15099 rule that complex cavities with small throats should be subdivided; however, our data suggest that cavities with throats smaller than seven millimeters (mm) should be subdivided, in contrast to the ISO 15099 rule, which places the break point at five mm. The agreement between CFD modeling results and the results of the simplified models is moderate. The differences in results may be a result of the underlying ISO correlations being based on studies where cavity height/length (H/L) aspect ratios were smaller than 0.5 and greater than five (with linear interpolation assumed in between). The results presented here are for horizontal frame members because convection in vertical jambs involves very different aspect

ratios that require three-dimensional CFD simulations. Ongoing work focuses on quantifying the exact effect on window thermal performance indicators of using the ISO 15099 approximations in typical real window frames.

INTRODUCTION

The frame is an important part of a fenestration product. In a window with a total area of 1.2×1.2 m^2 and a frame with a width of 10 cm, the frame occupies 30 percent of the window's total area. If the total area of the window is increased to 2.0×2.0 m^2, the same frame occupies 19 percent of the total area. When rating a fenestration product, engineers area-weight the thermal performance of the different parts of the product to determine a single number that describes the entire product. Thus, to be able to accurately calculate a product's thermal performance, engineers need models that accurately describe the thermal performance of each part of the product or accurate measurements of actual thermal performance. Because actual measurement is expensive, use of accurate models is preferable.

A significant body of research has focused on heat-transfer effects in glazing cavities. The primary goal of that work has been to develop accurate correlations for natural convection effects inside multiple-pane windows (Batchelor 1954, Eckert and Carlson 1961, Hollands et al. 1976, Raithby et al. 1977, Berkovsky and Polevikov 1977, ElSherbiny et al. 1982, Shewen et al. 1996, Wright 1996, and Zhao 1998). Less research has been conducted on heat transfer in window frames that have internal cavities. This is an important issue for high-performance window frames because cavities are a primary area where frame heat transfer can be minimized (the thermal conductivity of solid framing materials is another key area). In window frames with internal cavities, the heat-transfer process involves a combination of conduction, convection, and radiation. To fully describe heat transfer through these window frames, it would be necessary to

simulate fluid flow to determine the convection effects and to use either view-factors or ray-tracing techniques to determine the radiation effects inside the cavities. However, these types of simulations and techniques are rarely undertaken because they require significant computational resources and modeling efforts. Instead, air cavities in window frames are treated like solid materials that have an effective conductivity (Standaert 1984, Jonsson 1985, Carpenter and McGowan 1989); that is, conduction, convection, and radiation effects are combined into a single effective conductivity. With this single value, standard conduction simulation software can find the insulation value or thermal transmittance (U-value) of the frame using the same procedure as is used for solid window frames without internal cavities. The proposed standards ASHRAE 142P, prEN ISO 10077-2, and ISO 15099 (see ASHRAE 1996, CEN 2001, and ISO 2002, respectively) prescribe methods of this type for finding the thermal transmittance of window frames. To represent the air flow in frame cavities, various sources prescribe rules for subdividing cavities at points where their dimensions are smaller than a specified minimum. NFRC (Mitchell et al. 2003) and ISO 15099 indicate that cavities are to be divided at points when their dimensions are less than five millimeters (mm), and prEN ISO 10077-2 specify that cavities with one dimension not exceeding two mm or subareas of cavities with interconnection whose size does not exceed two mm should be divided into separate subcavities (here, the term “subarea” and “subcavity” is used for parts of a larger cavity that can naturally be separated from the larger cavity based on its geometric configuration). No research basis is given for the values used in these rules. The standards also differ in their rules for converting non-rectangular (or irregular) cavities into equivalent rectangular cavities whose convection and radiation correlations are assumed to be the same as the correlations for the original irregular cavity. ISO 15099 and prEN ISO 10077-2 specify that irregular cavities should be transformed into rectangular cavities so that the areas and aspect ratios of the original irregular cavity and the new rectangular cavity are

equal. ASHRAE 142P specifies that irregular cavities should be transformed into rectangular cavities using a bounding rectangle. The aspect ratios and the total heights and widths of the original irregular cavity and the new rectangular cavity should be equal. (The total heights and widths will most likely not be equal under ISO 15099 and prEN ISO 10077-2.)

In this paper, we focus on convective heat transfer in frame cavities; problems related to dividing cavities and transforming irregular cavities into rectangular cavities are addressed. Computational fluid dynamics (CFD) and conduction simulations were conducted for this study. In the conduction simulations, an effective conductivity was used to account for both conduction and convection in frame cavities. In a companion paper the U-values of complete window frames with internal cavities are studied.

GEOMETRIES STUDIED

The air cavities studied are shown in Figure 1. The particular cavities were chosen to represent air cavities that can be found in real window frames. The cavities are identified as H-cavity, L-cavity and C-cavity (left to right in Figure 1). H-cavity is square with two solid fins protruding into it. Measurements and temperature differences simulated for the cavities are shown in Tables 1 to 3. Because the cavities are simulated in two dimensions, the results are valid for horizontal frame members. CFD results that are valid for jamb sections require simulations in three dimensions.

Table 1. Cavity measures and temperatures for the H-cavity.

ID	L_v [mm]	L_h [mm]	L_a [mm]	L_f [mm]	T_H [ºC]	T_C [ºC]
H1	30	30	30	-	15	-10
H2	30	30	20	2	15	-10
H3	30	30	15	2	15	-10
H4	30	30	10	2	15	-10
H5	30	30	7	2	15	-10

H6	30	30	5	2	15	-10
H7	30	30	3	2	15	-10
H8	30	30	0	2	15	-10
H9	30	30	30	-	15	5
H10	30	30	20	2	15	5
H11	30	30	15	2	15	5
H12	30	30	10	2	15	5
H13	30	30	7	2	15	5
H14	30	30	5	2	15	5
H15	30	30	3	2	15	5
H16	30	30	0	2	15	5

Table 2. Cavity measures and temperatures for the L-cavity.

ID	L_v [mm]	L_h [mm]	L_{h1} [mm]	L_a [mm]	T_H [ºC]	T_C [ºC]
L1	30	30	10	15	15	-10
L2	30	30	10	10	15	-10
L3	30	30	10	7	15	-10
L4	30	30	10	5	15	-10
L5	30	30	10	3	15	-10
L6	30	30	10	15	15	5
L7	30	30	10	10	15	5
L8	30	30	10	7	15	5
L9	30	30	10	5	15	5
L10	30	30	10	3	15	5

Table 3. Cavity measures and temperatures for the C-cavity.

ID	L_v [mm]	L_h [mm]	L_{h1} [mm]	T_H [ºC]	T_C [ºC]
C1	20	30	10	15	-10
C2	20	30	10	15	5
C3	10	30	10	15	-10
C4	10	30	10	15	5

NUMERICAL PROCEDURE

The simulations were performed with a CFD code (Fluent 1998) and THERM 5.2.04 (Finlayson et al. 1998). Double precision was used for both codes. THERM uses a finite-element

approach to solve the conduction heat-transfer equation. The CFD code uses a control-volume method to solve the coupled heat and fluid-flow equations. Only natural convection is simulated; radiation effects are not addressed. In the CFD simulations, incompressible and laminar flow are assumed, viscous dissipation is not addressed, and all thermophysical properties are assumed to be constant except for the buoyancy term of the y-momentum equation where the Boussinesq approximation is assumed. The Semi-Implicit Method for Pressure-Linked Equations Consistent (SIMPLEC) was used to model the interaction between pressure and velocity. The energy and momentum variables at cell faces were found by using the Quadratic Upstream Interpolation for Convective Kinetics (QUICK) scheme. In addition, the CFD code uses central differences to approximate diffusion terms and relies on the PREssure Staggering Option scheme (PRESTO) to find the pressure values at the cell faces. PRESTO is similar to the staggered grid approach described by Patankar (1980). Convergence is determined by checking the scaled residuals and ensuring that they are less than 10^{-5} for all variables, except for the energy equation, in which the residuals have to be less than 10^{-6}.

A quadrilateral grid was used for all cavities. Some grid sensitivity tests were performed for the H- and C-cavities. The L-cavity was assumed to behave similarly to the H-cavity with respect to grid density; therefore, the same grid density was used for the L-cavity as for the H-cavity. For the H-cavity, the grid size was varied between 0.5 mm and 0.06 mm where the first size results in 3,600 nodes and the latter size results in 249,999 nodes. For the C-cavity, grid sizes of 0.5 mm, 0.1 mm, and 0.05 mm were tested, resulting in 2,369, 28,919, and 227,195 nodes, respectively. An interval size of 0.1 mm was found to be sufficient for all cavities. Reducing the grid sizes to 0.06 mm for the H-cavity and 0.05 mm for the C-cavity resulted in changes of heat fluxes of less than 0.5 percent.

The conduction simulations were performed using a special version of THERM 5.2.04 in which the radiation calculation in frame cavities was disabled, which allowed us to compare the convection effects with the CFD calculations. The quadrilateral mesh is automatically generated. Refinement was performed in accordance with section 6.3.2 b. of ISO 15099. The Energy Error Norm was less than 10 percent in all cases, which results in an error of less than one percent in the thermal transmittance of the cavities. The temperatures on the boundaries of the cavities were fixed using a very large combined convective and radiative film coefficient (h = 99,900 W m^{-2} K^{-1}). The resulting cavity wall temperatures were within 0.01°C of the desired temperatures. For more information on the THERM algorithms refer to Appendix C in Finlayson et al. (1998).

Boundary Conditions and Material Properties

The air properties used in the CFD simulations are calculated at mean temperature, $(T_H+T_C)/2$, and atmospheric pressure, P = 101325 Pa, and are shown in Table 4. The gravity is set to 9.8 m s^{-2}. Constant temperature boundary conditions are specified at all vertical walls and at the sloped wall of the C-cavity (see Figure 1). All horizontal walls are adiabatic. The conductivity of the fin in the H-cavity is set to 0.25 W m^{-1} K^{-1}.

Table 4. Air properties used in the CFD simulations.

$(T_H+T_C)/2$ [C]	[W m^{-1} K^{-1}]	c_p [J kg^{-1} K^{-1}]	[kg m^{-1} s^{-1}]	[kg m^{-3}]	[K^{-1}]
2.5	0.024253	1005.2	1.7357 10^{-5}	1.2807	3,6278 10^{-3}
10	0.024817	1005.5	1.7724 10^{-5}	1.2467	3,5317 10^{-3}

RESULTS

Heat Transfer Rates for the H-cavity and the L-cavity

Heat fluxes for different gap openings, L_a, are plotted for the H-cavity and L-cavity. For the H-cavity, the heat flux is found from:

$$q = Q/L_v \quad ,$$

where Q is the heat flow through the warm side of the cavity and L_v is the height of the cavity (equal to 30 mm for all H-cavities). For the L-cavity, the total heat flux is calculated according to:

$$q_{Total} = (Q_{TH} + Q_{Tm})/L_v \quad , \quad q_{TH} = Q_{TH}/L_a \quad , \text{ and } q_{Tm} = Q_{Tm}/L_{Tm}$$

where Q_{TH} and Q_{Tm} are the heat flows through the parts of the cavity having temperatures T_H and T_m, respectively, and L_a and L_{Tm} are the lengths of the respective parts of the cavity. L_{Tm} is equal to the height of the cavity (L_v) minus L_a.

Figure 2 and Figure 3 show the heat flux from the CFD calculations through the warm wall of the H-cavity as a function of gap opening, L_a, for temperature differences between the warm and cold walls of 10ºC and 25ºC, respectively. The vertical axis shows the heat flux in W/m^2, and the horizontal axis shows the gap opening in millimeters.

Figure 4 and Figure 5 show the heat fluxes from the CFD simulation through the cavity walls with temperatures T_H and T_m and the total fluxes for the L-cavity as function of gap opening for temperature differences between the warm and cold surfaces of 10ºC and 25ºC, respectively. The vertical axis shows the heat flux in W/m^2, and the horizontal axis shows the gap opening, L_a, in millimeters.

Stream Contours

Insight into the airflow in frame cavities may also be gained by looking at the stream contours for the different cavities. Figure 6 displays stream contours for the H-cavity. The diagrams in the left column display results for the cases in which the temperature difference between the warm and cold walls is 10ºC, and the right diagrams show results where the temperature difference is 25ºC. Each row includes results for different gap openings, L_a (see the geometry to the left in Figure 1). The magnitude of the stream contours is set automatically by the CFD program, and the contour lines are distributed at even intervals between the maximum and minimum values for each case.

Figure 7 displays stream contours for the various versions of the L-cavity. The left column diagrams show results for the cases where the temperature difference between the warm and cold walls is 10ºC, and the right diagrams show results where the temperature difference is 25ºC. Each row includes results for different gap openings, L_a.

Figure 8 shows the stream contours for the versions of the C-cavity. The left and right columns of graphs display results where the temperature differences are 10ºC and 25ºC, respectively. Each row corresponds to a fixed cavity height, L_v. The various diagrams show that there is little circulation close to the corners with sharp angles. By making tangents to the outer stream contour line for each cavity (close to the sharp corners), we find the measures 6.6, 6.3, 8.8, and 7.5 mm for the lengths of the tangents (from left to right, line by line).

Comparison of CFD and ISO 15099 Convection Correlations

Although there are several correlations and procedures for finding effective conductivity, we focused on those presented in ISO 15099. To check the accuracy of these correlations and procedures, we compared the CFD results with conduction simulations based on ISO 15099.

Results for H-cavity are shown in Figures 9 and 10 for the cases where the temperature differences between the warm and cold surfaces are 10° and 25°C, respectively. Results for the L-cavity are shown in Figures 11 and 12 for the cases where the temperature differences between the warm and cold surfaces are 10° and 25°C, respectively. The vertical axis shows the heat flux in W/m^2, and the horizontal axis shows the gap opening, L_a, in millimeters. The graphs are titled as follows:

"CFD" signifies the results from the CFD simulation.

"THERM 5mm-Rule" denotes the heat fluxes that were calculated in THERM 5.2.04 according to the proposed standard ISO 15099; for these examples, the air cavity was divided when the distance between two opposite surfaces was smaller than five mm. Thus, for the H-cavity, the air cavity was divided when the interconnection formed by the fins was smaller than five mm, resulting in three separate air cavities. (If the distance between the fins in the air cavity was equal to 5 mm or more there is no division.)

"THERM Division" identifies results where the air cavity in all the various sections was divided (even if the gap opening is larger than the five-mm limit set in ISO 15099). For the H-cavity this results in three separate air cavities for which THERM computes an equivalent conductivity. The $L_a = 0$ result indicates that the two fins are joined, so two separate air enclosures are separated by a solid fin in the middle.

"THERM No-Division" means that no divisions are made, even for cavities where the interconnection is smaller than five mm.

Table 5 shows heat fluxes for the C-cavity as function of temperature difference and air cavity height. The table includes, in addition to CFD results, results from conduction simulations

where an effective conductivity was used to account for conduction and convection. These were carried out both with a five-mm vertical division of the air cavity in the sharp angle of the cavity (column labeled "5-mm-Rule") and no division of the air cavity (column labeled "No-Division"). Results are included for temperature differences between the warm and cold walls equal to 10º and 25ºC.

Table 5. Comparisons of heat fluxes for the C-cavity.

	Heat Flux [W m^{-2}]					
	T = 10 ºC			**T = 25 ºC**		
L_v [mm]	**CFD**	**No Division**	**5-mm-Rule**	**CFD**	**No Division**	**5-mm-Rule**
10	23.65518	19.996	23.063	87.3778	63.9525	87.4525
20	31.57198	28.272	20.195	105.04675	123.675	71.7

DISCUSSION

As noted in the introduction to this paper, various rules address the break point at which to divide air cavities in window frames. In this section, the results from the previous section are analyzed in detail to determine the point at which frame air cavities should be divided. We also discuss the agreement between the CFD results and the procedures in ISO 15099 for calculating heat flow through air cavities of window frames.

Heat Transfer Rates and Contour Plots – Cavity Division Rule

Heat-transfer rates and stream contour plots were reported above for all cavities. Figures 2 and 3 display the heat fluxes for the H-cavity as a function of gap opening for ΔT equal to 10° and 25 °C, respectively. In both cases, we find that the heat flow is fairly constant for gap openings less than five to seven mm. When the gap opening increases from seven to ten mm, the increase in heat flux is more pronounced. These results suggest that air cavities should be divided when the gap opening is less than seven mm. However, when the temperature difference between

the warm and cold walls increases, heat flux increases for smaller gap openings. For the L-cavity, we find that the total heat flux is fairly constant for all gap openings, but when we look at the part fluxes through the surfaces having temperatures of T_H and T_m, we find that these fluxes changes more when the gap opening is larger than five to seven mm.

The stream contour diagrams for H-cavity, Figure 6, show that the airflow is separated between the two subcavities primarily for gap openings smaller than or equal to five mm. For a gap opening equal to seven mm, there is some airflow between the two subcavities. The graphs show that the air exchange between the subcavities increases when the gap opening is larger than seven mm. Similar observations may be made for the L-cavity (Figure 7). Little airflow occurs in the small subcavity compared to the airflow in the higher part of the cavity, as long as the height of the subcavity, L_a, is less than or equal to five mm. When the height of the subcavity increases to seven mm and larger, air circulates throughout the entire cavity.

For the C-cavity, Figure 8, the contour plots show that there is limited air circulation in the sharp corner of the cavity. As reported in the Results section above, if we make tangents to the outer stream contour line for each cavity, the tangent lengths measure 6.6, 6.3, 8.8, and 7.5 mm (from left to right, line by line in Figure 8). Thus, such cavities may best be divided at the sharp corners when the distance between opposing walls is less than about six mm.

Based on the CFD simulations describe above, it seems that a "five- to seven-mm rule" should be applied when dividing air cavities in window frames.

Comparison of CFD and ISO 15099 Convection Correlation

ISO 15099 includes convection correlations and rules for treating air cavities in window frames. These rules specify that if the shortest distance between two opposite surfaces is smaller than five mm, then the frame cavity should be split into subcavities at this "throat" region.

Figures 9 to 12 and Table 5 show a comparison between CFD and conduction simulation results both with and without splitting of air cavities into subcavities. Although a few numbers are comparable, most are not. Nonetheless, for the H-cavity in Figures 9 and 10, we find that the shape of the curves is somewhat similar. The graphs for L-cavity differ more strongly. The maximum deviations between the CFD and THERM Five-mm Rule (ISO 15099) results are 27 percent and 41 percent for the H-cavity with ΔT equal to 10° and 25°C, respectively. For the L-cavity the comparable results are 31 and 60 percent, respectively.

It is important to note that for the H-cavity, there are two reasons for the reduction of heat flux as the gap opening decreases from 30 mm to five mm. One is the reduction of size of the air cavity caused by the added fin material; the other is the decrease in effective temperature across the cavity even though the temperatures of the hot and cold walls of the original cavity are fixed. The effective temperature decreases because, according to ISO 15099, the temperature of each wall in the original irregular cavity is assigned to a wall in the new rectangular cavity depending on the orientation of the normal vector of the original wall. Thus, the irregular cavity's vertical fin surfaces are divided between the hot and cold walls in the new rectangular cavity, and new warm and cold wall temperatures are then calculated. Because the fins are in the middle of the cavity and therefore have a temperature approximately equal to the average of T_H and T_C, the result will be a reduced temperature difference across the cavity. This again reduces the effective conductivity of the enclosure.

Two of the H-cavity configurations studied did not include division of air cavities to calculate heat flux. These are the H-cavity with no fins protruding into the cavity (L_a = 30 mm in Figures 9 and 10) and the H-cavity with one fin separating two air enclosures (L_a = 0 in Figures 9 and 10). The former results in a simple square cavity while the latter results in two cavities with height to length aspect ratio (H/L) of 30/14 (≈ 2.14) separated by two-mm-thick solid fin. For

these cavities, no large differences would be expected between the CFD and the ISO 15099 correlations. Also, the square air cavity results do not differ significantly for the ΔT = 25°C case, but they do differ significantly for the ΔT = 10 °C case. There are also large differences between the CFD and the ISO 15099 results for the configuration where one fin separates two enclosures (both for ΔT = 10° and 25°C, Figures 11 and 12). The reason for these differences is the lack of accuracy of the horizontal heat-flow natural convection correlations between H/L = 0.5 and H/L = 5, in which the equivalent conductivity is found by interpolation (see ISO 15099). The good agreement for the no-fin configuration where ΔT = 25°C is mainly a result of chance. The lack of accuracy for the ISO 15099 convection correlation has been noted by Gustavsen (2001). If the natural convection correlations for frame cavities were more accurate, greater agreement in results would be expected. In addition to above modeled cavities, we conducted an extra study to evaluate the accuracy of the convection correlation in ISO 15099. We used a cavity 30 mm high and 14 mm wide containing only air. This cavity has the same dimensions as the two air cavities in the 30 by 30 mm cavity with a two-mm-wide fin in the middle. Temperatures of -10° and 2.5°C were used. The CFD and THERM simulations resulted in 41.36 and 27.94 W m^{-2}, respectively. These figures equal Nusselt numbers of 1.95 from the CFD simulation and 1.32 from THERM (ISO 15099).

The fluxes for the C-cavity are shown in Table 5. For the cavities that have heights (L_v) of 10 mm, we see that the heat flux for the divided cavity is greater than for the undivided cavity. This seems unexpected because dividing frame cavities usually reduces convection, so a division would be assumed to produce a smaller heat flux. However, the increased heat flux after division of the air enclosure in this case may be explained by the change in height to length aspect ratio (H/L) of the cavities from before the division of cavity to after. For the original cavity, the height to length aspect ratio is smaller (H/L = 0.33) than for the largest cavity in the divided case (H/L =

0.5). For small aspect ratios, natural convection is suppressed, so lower fluxes are found for the undivided cases. For these cases (L_v = 10 mm), we also find good agreement between CFD- and divided-cavity results (the ISO 15099 convection correlations for H/L < 0.5 are assumed to be correct because they are based on analytical considerations). For the C-cavities with a height of 20 mm, we find that dividing the cavity reduces the heat flux, but this does not bring the results closer to the CFD results. Here all cavities have aspect ratios within the interpolation range of the ISO 15099 correlation.

CONCLUSIONS

Based on our results and discussion, we can conclude that irregular-shape frame cavities should be divided at points where their dimensions are in the range of five to 10 mm; analyzing our stream contour plots suggests that seven mm is an appropriate break point. This rule should apply to any constrictions in cavity volume, even in triangular cavities. The impact of frame cavity heat transfer on the frame U-value is likely to be larger for highly insulating window frames, which usually have many air cavities. To assess the effect on the U-value of an actual window frame of using seven mm as the break point for dividing cavities, another paper will be published using the same two calculation methods as in the current study. The heat flux results from CFD and conduction simulations based on ISO 15099 show good agreement in the case of certain cavity configurations. For other aspect ratios, the difference between the two calculation methods is quite significant even for simple rectangular cavities. This difference is a result of the limitation in the linear interpolation that is used in ISO 15099 for frame cavities with an aspect ratio between 0.5 and five. Future work will focus on improving the natural convection correlation for these aspect ratios.

FUTURE RESEARCH

In addition to the topics mentioned above, studies should be undertaken to determine how effective the radiation correlation proposed in ISO 15099 is for irregular cavities.

ACKNOWLEDGMENTS

This work was supported by Hydro Aluminum and the Assistant Secretary for Energy Efficiency and Renewable Energy, Office of Building Technology, State and Community Programs, Office of Building Systems of the U.S. Department of Energy under Contract No. DE-AC03-76SF00098. We would like to thank Nan Wishner, Lawrence Berkeley National Laboratory, for editorial assistance.

REFERENCES

ASHRAE 1996. *Draft BSR/ASHRAE Standard 142P - Standard method for determining and expressing the heat transfer and total optical properties of fenestration products*. Atlanta: American Society of Heating, Refrigerating and Air-conditioning Engineers Inc.

Batchelor, G.K. 1954. Heat transfer by free convection across a closed cavity between vertical boundaries at different temperatures. *Quarterly Applied Mathematics*, Vol. 12, pp. 209-233.

Berkovsky, B.M. and V.K. Polevikov. 1977. Numerical study of problems on high-intensive free convection. In: *Heat Transfer and Turbulent Buoyant Convection* (D.B. Spalding and N. Afgan, editors), Vol. II, pp. 443-455. Washington: Hemisphere Publishing Corporation.

Carpenter, S.C. and A.G. McGowan. 1989. Frame and spacer effects on window U-value. *ASHRAE Transactions*, Vol. 95, pp. 604-608.

CEN 2001. *prEN ISO 10077-2 - Thermal performance of windows, doors and shutters - Calculation of thermal transmittance - Part 2: Numerical method for frames.* Brussels: European Committee for Standardization.

Eckert, E.R.G. and W.O. Carlson. 1961. Natural convection in an air layer enclosed between two vertical plates with different temperatures. *International Journal of Heat and Mass Transfer*, Vol. 2, pp. 106-120.

ElSherbiny, S.M., G.D. Raithby, and K.G.T. Hollands. 1982a. Heat transfer by natural convection across vertical and inclined air layers. *Journal of Heat Transfer. Transactions of the ASME*, Vol. 104, pp. 96-102.

Finlayson, E., R. Mitchell, D. Arasteh, C. Huizenga, and D. Curcija. 1998. *THERM 2.0: Program description. A PC program for analyzing the two-dimensional heat transfer through building products*. Berkeley: University of California.

Fluent 1998. *FLUENT 5 User's Guide*. Lebanon, UK: Fluent Incorporated.

Gustavsen, A. 2001. *Heat Transfer in Window Frames with Internal cavities*. Ph.D. Thesis. Trondheim: Department of Building and Construction Engineering. Norwegian University of Science and Technology.

Hallé, S., M.A. Bernier, A. Patenaude, and R. Jutras. 1998. The combined effect of air leakage and conductive heat transfer in window frames and its impact on the Canadian energy rating procedure. *ASHRAE Transactions*, Vol. 104, pp. 176-184.

Hollands, K.G.T., T.E. Unny, G.D. Raithby, and L. Konicek. 1976. Free convective heat transfer across inclined air layers. *Journal of Heat Transfer. Transactions of the ASME*, Vol. 98, pp. 189-193.

ISO 2002. *Proposed standard ISO/DIS 15099 - Thermal performance of windows, doors and shading devices - Detailed calculations*. Geneva: International Organization for Standardization.

Jonsson, B. 1985. *Heat transfer through windows. During the hours of darkness with the effect of infiltration ignored. Document D13:1985*. Stockholm: Swedish Council for Building Research.

Mitchell, R., C. Kohler, D. Arasteh, C. Huizenga, J. Carmody, and D. Curcija. 2003. *THERM 5/WINDOW 5 NFRC simulation manual*. Berkeley CA, USA: Lawrence Berkeley National Laboratory.

Patankar, S.V. 1980. *Numerical heat transfer and fluid flow*. Washington, D.C.: Hemisphere.

Raithby, G.D., K.G.T. Hollands, and T.E. Unny. 1977. Analysis of heat transfer by natural convection across vertical fluid layers. *Journal of Heat Transfer. Transactions of the ASME*, Vol. 99, pp. 287-293.

Shewen, E., K.G.T. Hollands, and G.D. Raithby. 1996. Heat transfer by natural convection across a vertical air cavity of large aspect ratio. *Journal of Heat Transfer. Transactions of the ASME*, Vol. 118, pp. 993-995.

Standaert, P. 1984. Thermal evaluation of window frames by the finite difference method. In: *Proceedings of Windows in Building Design and Maintenance*. Stockholm: Swedish Council for Building Research.

Wright, J. 1996. A correlation to quantify convective heat transfer between vertical window glazings. *ASHRAE Transactions*, Vol. 102, pp. 940-946.

Zhao, Y. 1998. *Investigation of heat transfer performance in fenestration system based on finite element methods*. Ph.D. dissertation. Massachusetts: Department of Mechanical and Industrial Engineering, University of Massachusetts, Amherst.

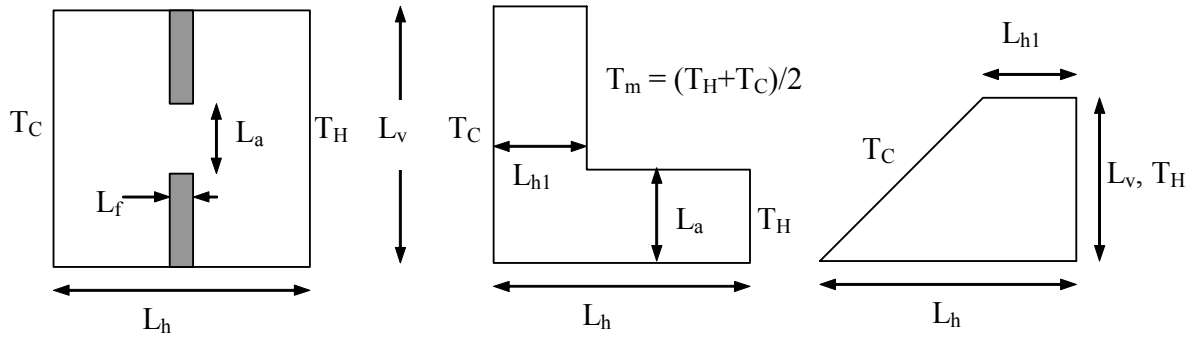

Figure 1 Schematics of cavities simulated. From left to right we have the H-cavity, L-cavity and the C-cavity.

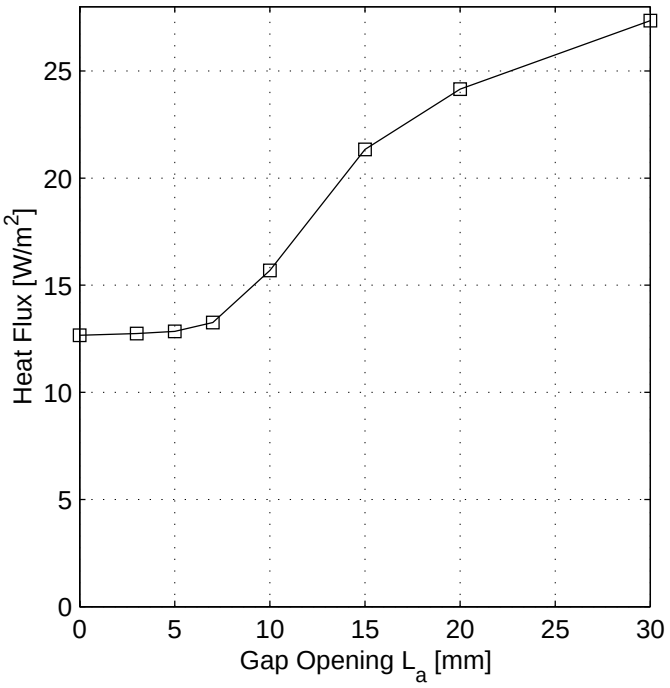

Figure 2. Graph of heat flux from the CFD simulation through warm side of the H-cavity as function of gap opening, L_a. The temperature difference between warm and cold surfaces is 10 ºC.

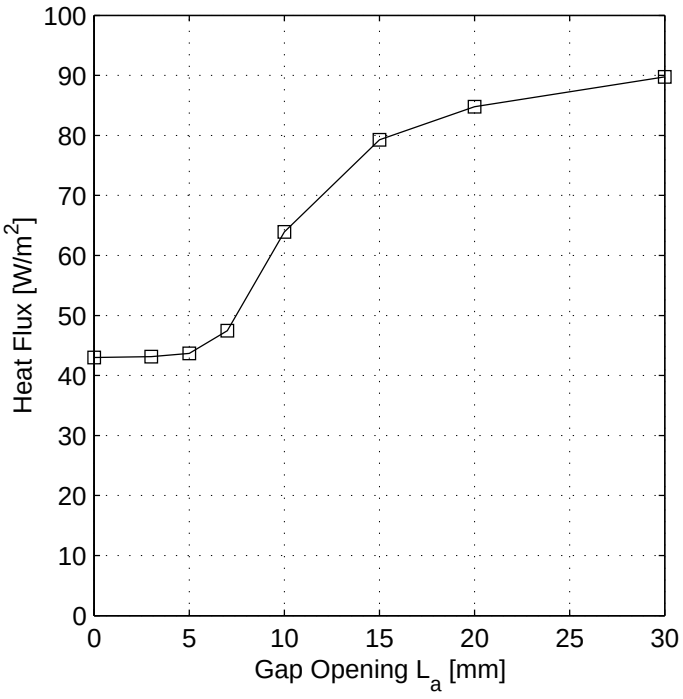

Figure 3. Graph of heat flux from the CFD simulation through warm side of the H-cavity as function of gap opening, L_a. The temperature difference between warm and cold walls is 25 ºC.

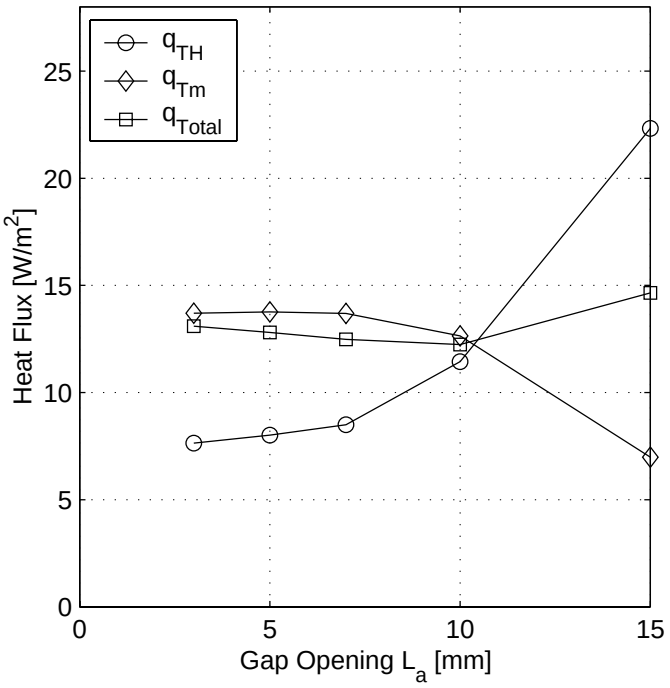

Figure 4. Graph of the heat fluxes from the CFD simulation through the cavity walls with temperatures T_H and T_m, and the sum of the fluxes for the L-cavity as function of gap opening, L_a. The temperature difference between warm and cold surfaces is 10 ºC.

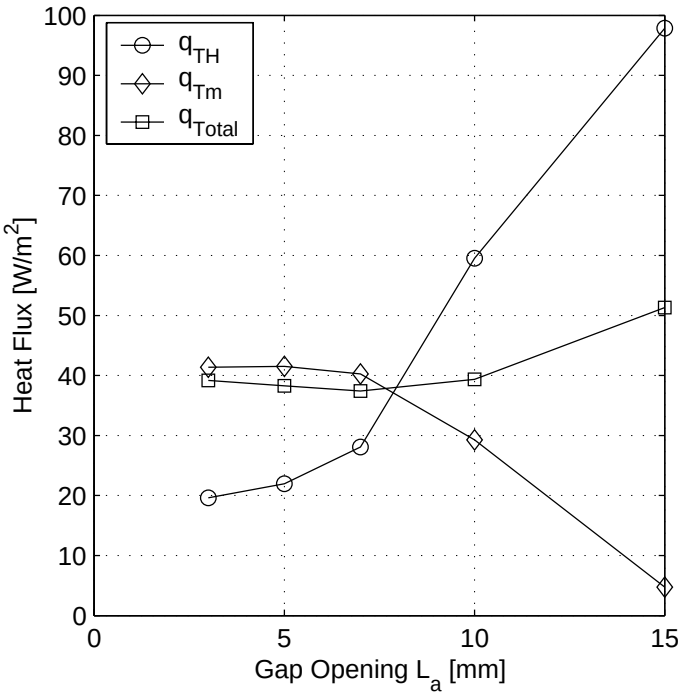

Figure 5. Graph of the heat fluxes from the CFD simulation through the cavity walls with temperatures T_H and T_m, and the sum of the same fluxes for the L-cavity as function of gap opening, L_a. The temperature difference between warm and cold surfaces is 25 ºC.

	T = 10 ºC	T = 25 ºC
L_a = 3 mm	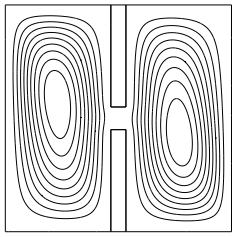	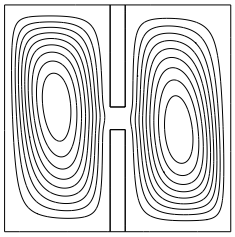
L_a = 5 mm	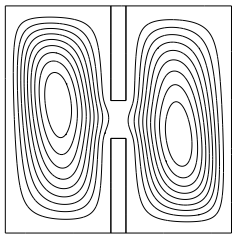	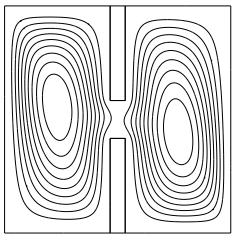
L_a = 7 mm	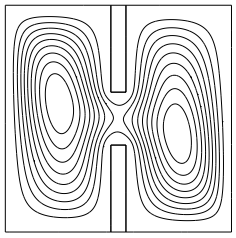	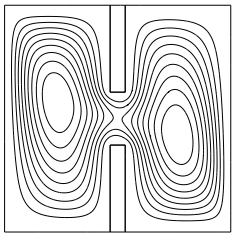
L_a = 10 mm	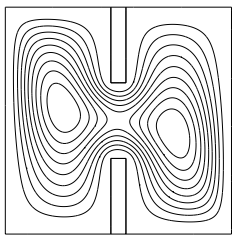	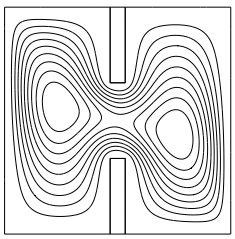
L_a = 15 mm	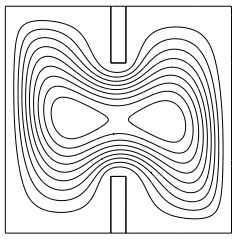	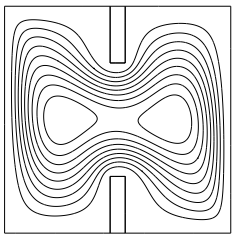
L_a = 20 mm	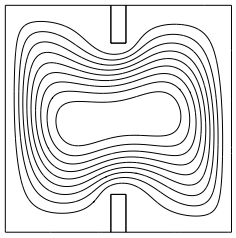	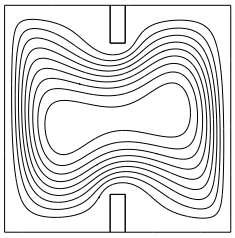

Figure 6. The figure shows stream contours for the H-cavities. L_a is the size of the gap opening, and ΔT is the difference between the hot and cold wall temperatures, reported in ºC.

	T = 10 ºC	T = 25 ºC
L_a = 3 mm	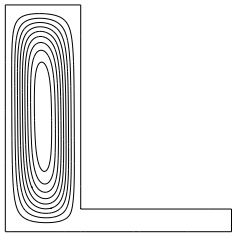	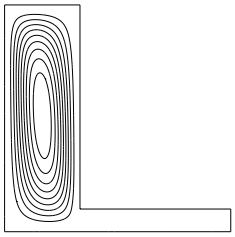
L_a = 5 mm	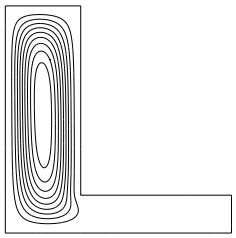	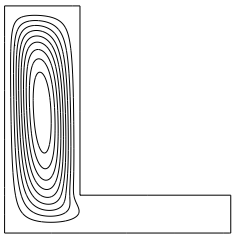
L_a = 7 mm	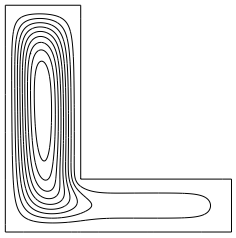	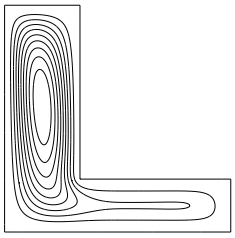
L_a = 10 mm	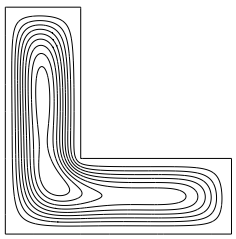	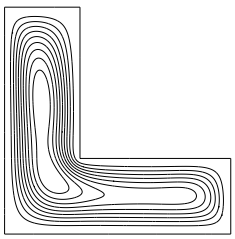
L_a = 15 mm	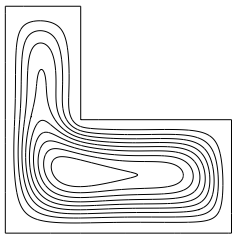	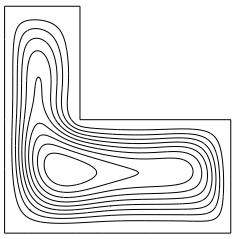

Figure 7. Stream contours for the L-cavities. L_a is the size of the gap opening, and ΔT is the difference between the hot and cold wall temperatures, reported in ºC.

	T = 10 ºC	T = 25 ºC
L_v = 10 mm	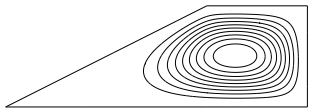	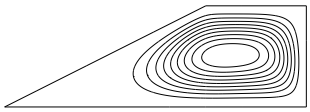
L_v = 20 mm	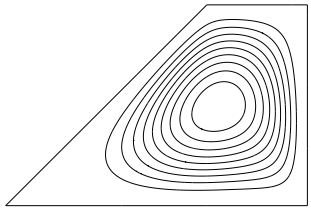	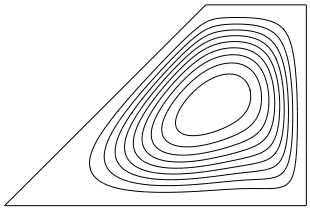

Figure 8. The figure shows stream contours for the C-cavities for different temperature differences; T. L_v is the height of the cavity.

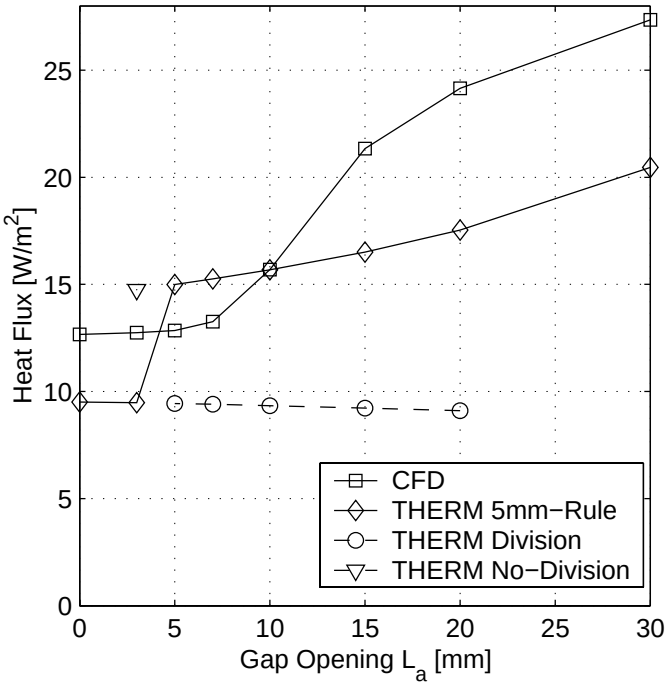

Figure 9. Comparison of heat fluxes from CFD and conduction simulations for the H-cavity as a function of gap opening, L_a. The temperature difference between the warm and the cold surfaces is 10 °C.

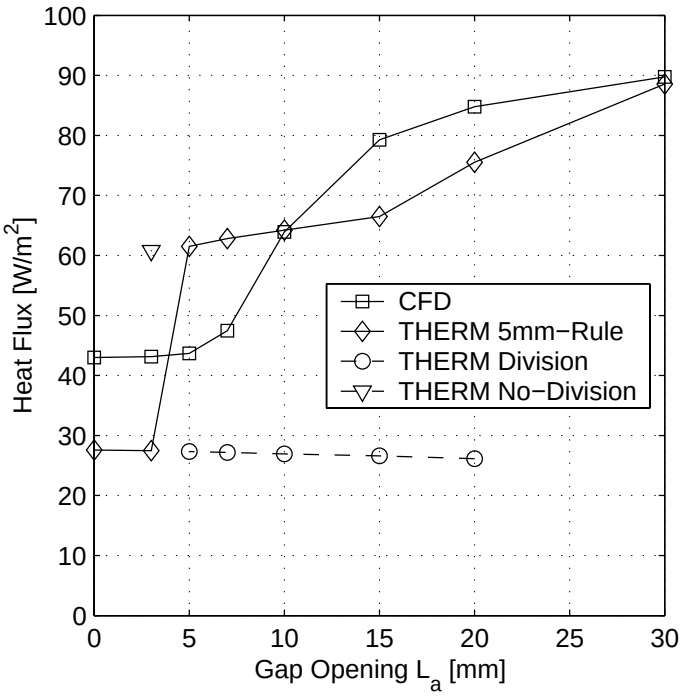

Figure 10. Comparison of heat fluxes from CFD and conduction simulations for the H-cavity as a function of gap opening, L_a. The temperature difference between the warm and the cold surfaces is 25 °C.

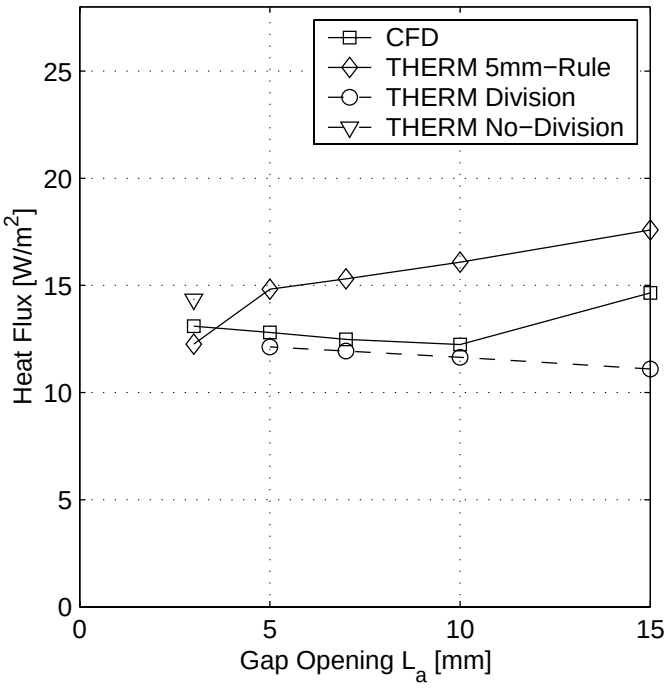

Figure 11. Comparison of heat fluxes from CFD and conduction simulations for the L-cavity as a function of gap opening, L_a. The temperature difference between the warm and the cold surfaces is 10 °C.

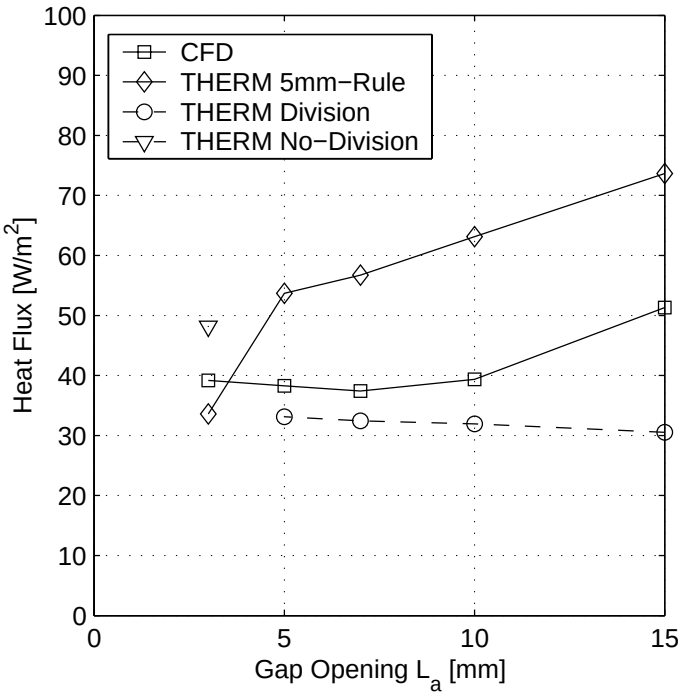

Figure 12. Comparison of heat fluxes from CFD and conduction simulations for the L-cavity as a function of gap opening, L_a. The temperature difference between the warm and the cold surfaces is 25 °C.